Molecular Crystals and Liquid Crystals Science and Technology. Section A. Molecular Crystals and Liquid Crystals

Publication details, including instructions for authors and subscription information:
http://www.tandfonline.com/loi/gmcl19

X-Ray Diagnostics of the Layered Organic/Inorganic Nanostructures

A. G. Fedorov [a]

[a] Institute for Single Crystals, NAS of Ukraine, Lenin Ave., 60, 61001, Kharkov, Ukraine

Version of record first published: 24 Sep 2006

To cite this article: A. G. Fedorov (2001): X-Ray Diagnostics of the Layered Organic/Inorganic Nanostructures, Molecular Crystals and Liquid Crystals Science and Technology. Section A. Molecular Crystals and Liquid Crystals, 361:1, 251-256

To link to this article: http://dx.doi.org/10.1080/10587250108025746

Mol. Cryst. and Liq. Cryst., 2001, Vol. 361, pp. 251-256
Reprints available directly from the publisher
Photocopying permitted by license only

X-Ray Diagnostics of the Layered Organic / Inorganic Nanostructures

A.G. FEDOROV

Institute for Single Crystals, NAS of Ukraine, Lenin Ave., 60, 61001 Kharkov, Ukraine

Possibilities of X-ray diffraction to examine the structure of organic and inorganic multilayers are discussed on examples of semiconductor superlattice and lead stearate multilayer.

Keywords: multilayer; X-ray diffraction; profile

The inherent carrier transport properties of the layered organic compositions are dependent on the more or less degree of its structure ordering. X-ray diffraction offers the convenient opportunities to examine the structure of the ordered scattering objects, due to highly developed methods and formalism. Here will be discussed the possibilities of X-ray diffraction in examining of the multilayers (ML).

Some kind of ML is the single crystalline semiconductor superlattice grown epitaxially on the orienting substrate. X-ray diffraction on such object gives the Bragg reflection lapped with satellites (Fig. 1a). The appearance of satellites is due to the additional comparely large periodicity of the pile of layers. Disposition of satellites is defined by the superlattice period and their relative intensity is dependent from the difference in electron density of the layers.

Thin ML film built of organic molecules has a slight scattering ability being constructed of the light elements, so it does not exhibit appreciable Bragg reflection. But ordering of the layers in normal direction allows to use the low angle diffraction to examine the structure. At this mode the diffraction pattern appears due to the periodical distribution of the dielectric constant in a film, so it is based on Fresnel interferention. Of course, structure of the single crystalline superlattice mentioned above allows to observe the low angle diffraction too for the

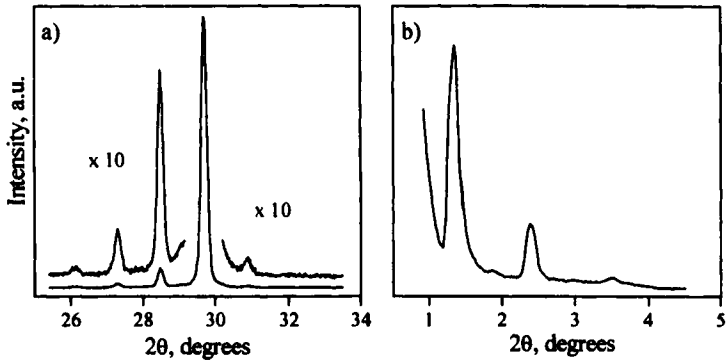

FIGURE 1. X-ray diffraction pattern of EuS-PbSe superlattice. Bragg diffraction (a) and low angle diffraction (b). Period of structure 84 Å.

same reason, – periodic distribution of electron density. The low angle diffraction pattern of the same specimen of semiconductor superlattice is shown on Fig. 1b.

Low angle diffraction pattern from the organic/inorganic composed ML is shown on Fig. 2. Specimen was prepared by consecutive deposition of 40 lead stearate layers onto the silicon substrate with Langmiur-Blodgett technique. High ordering in the normal to surface direction allows to obtain more then 20 reflections owing to the presence of strongly reflecting Pb-enriched layers. As the diffraction pattern represents the Fourier transform of the periodical distribution of electron density, so the inverse transform gives the profile of ML, in a case of symmetrical profile it is given by expression (1).

$$\rho(z) = \rho + \frac{2}{H}\sum_n A_n \cos\frac{2\pi n z}{H} \qquad (1)$$

In Eq. (1) H is ML period, z is the normal direction to surface. Expansion amplitudes A_n are the square roots of reflection intensities of corresponding number. Lead stearate ML profile restored by application of inverse Fourier transform to the diffraction pattern on Fig. 2 is shown on Fig. 3a. There are seen the area of increased electron density corresponding to the lead containing layer and a hollow connected with the

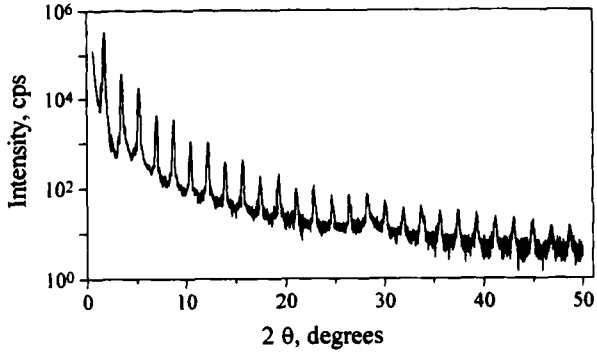

FIGURE 2. X-ray diffraction pattern of lead stearate 40-period multilayer. Period of structure 50 Å.

slight descent of electron density on the end of stearate molecule terminated with hydrogen atom. So the whole layer consists of two lead stearate molecules connected with their hydrogen terminated ends.

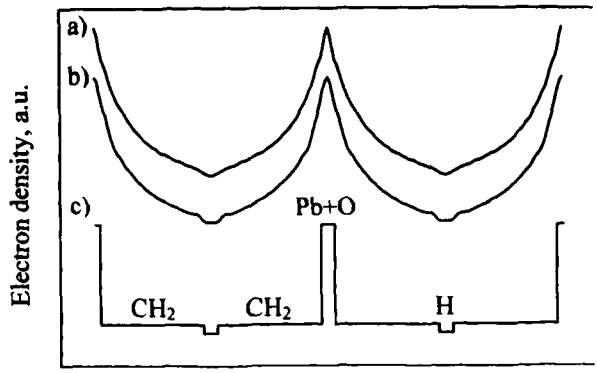

FIGURE 3. Restored electron density distribution (two periods shown) from experimental diffraction pattern (a), from simulated diffraction with Fresnel equations (b) and model lead stearate profile (c).

This is confirmed by the value of the structure period that match to the doubled length of stearate molecule. Refinement of the ML structure may be achieved using the numerical simulation based on Fresnel equations. Reflectivity of ML in X-ray waverange is given by the set of recurrent equations [1,2]

$$R_j = \frac{R_j^F + R_{j+1}\exp(2i\psi_{j+1}h_{j+1})}{1 + R_j^F R_{j+1}\exp(2i\psi_{j+1}h_{j+1})}, \quad R_j^F = \frac{\sqrt{\varepsilon_j - \sin^2\varphi_0} - \sqrt{\varepsilon_{j+1} - \sin^2\varphi_0}}{\sqrt{\varepsilon_j - \sin^2\varphi_0} + \sqrt{\varepsilon_{j+1} - \sin^2\varphi_0}}$$

Here R_j is the reflectivity from the interface of j-th and j+1-th layer counted from the border with substrate towards surface, R_j^F is the usual Fresnel reflectivity coefficient from the boundary of two media, $\psi_j = 2\pi/\lambda \sqrt{\varepsilon_j - \sin^2\varphi_0}$ and dielectric constant of j-th layer in X-ray waverange is determined as

$$\varepsilon_j = 1 - (e^2/mc^2)(\lambda^2/\pi)(\delta_j + i\gamma_j), \quad \delta_j = N_j f_j^{(1)}, \gamma_j = N_j f_j^{(2)} \qquad (2)$$

N_j is the mean atomic density and $f_j^{(1)}, f_j^{(2)}$ – mean atomic amplitudes of j-th layer. Calculated dependence of reflected intensity I = RR* versus angle of incidence φ_0 counted from the normal represents the simulation of the diffraction pattern which may be adjusted to experimental one with the values of layer thickness h and electron densities as fitting parameters. The result of simulation is shown on Fig. 3b.

The effect of heavy atoms contained in a layers is demonstrated on Fig. 4. There are shown the diffraction patterns of initially pure stearic acid and after introduction of Pb by treatment in $Pb(NO_3)_2$ solution. Appearance of the set of strong reflections denotes that lead ions are not distributed randomly in a matrix but occupy strictly confined places at the layer boundaries, so in this case we observe the increased ordering of the object after introduction of Pb ions.

Application of Fresnel equations to describe diffraction on the ML supposes that the ML possess the rectangular profile with pronounced abrupt interfaces. But really ML may not offer such ideal rectangular profile because some processes may smooth or distort the transitions from layer to layer as a consequence of diffusion, or formation of new phase, or others. In this case another approach is eligible that

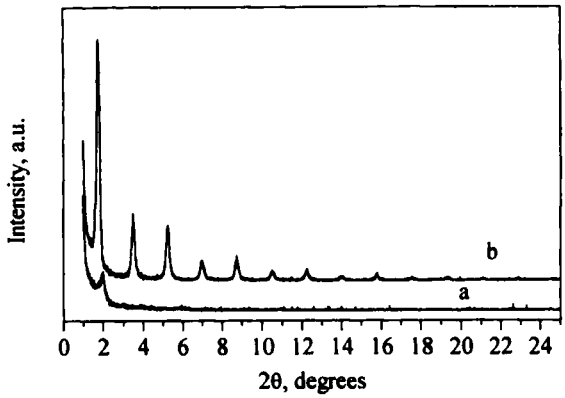

FIGURE 4. X-ray diffraction from pure stearic acid (a) and from the same specimen after treatment in $Pb(NO_3)_2$ solution (b)

allows to calculate diffraction for the object with arbitrary distribution of dielectric constant in the layers. This is possible by employing the direct solution of Maxwell equations for the layered medium [3, 4]

$$\frac{dR}{dz} = -2ik_0 R\sqrt{\varepsilon(z) - \sin^2\varphi_0} + (1 - R^2)\frac{\varepsilon'(z)}{4[\varepsilon(z) - \sin^2\varphi_0]}$$

Here $\varepsilon' = d\varepsilon / dz$. This Riccatti type equation being solved numerically gives the complex reflected amplitude in assigned angular range for the ML with dielectric constant distribution presented in any way, for example, as a Fourier series. Dielectric constant is given by expression (2), real and imaginary parts of atomic amplitudes $f^{(1)}$ and $f^{(2)}$ for particular substances may be found in [5] or downloaded from the site www–cxro.lbl.gov/optical_constants/asf.html. The example of implementation of this method is shown on Fig. 5 demonstrating the influence of diffusion intermixing on the diffraction pattern (on this and next figure the reflections from 2nd to 6th order are shown because the first order reflection always the most strong and not changes). It is seen the regular exponential decrease of reflection intensities, more fast for reflections with larger number. Moreover, the processes on the layer boundaries may not be obligely identical, so the asymmetrical profile

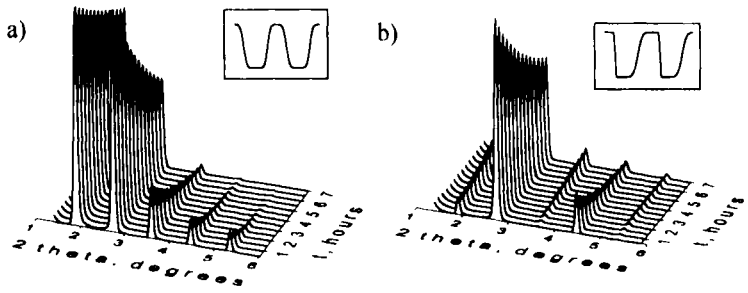

FIGURE 5. a) – the set of calculated diffraction patterns of the multilayer subjected to diffusion intermixing with diffusion coefficient $2.5 \cdot 10^{-19}$ cm^2/s. Final profile is shown on the inset; b) – calculated diffraction parrerns of the multilayer after simulated asymmetric diffusion intermixing with diffusion coefficients $2 \cdot 10^{-20}$ cm^2/s and $5 \cdot 10^{-19}$ cm/s on the sides of layer.

transformation may take place [6]. This gives another development of diffraction picture. A slight decrease of the layer symmetry leads to appearance and growth of formerly forbidden reflections.

Acknowledgements
This work was partly supported by INTAS grant # 96-0535

References

[1] A. V. Vinogradov and I. V. Kozhevnikov, *Proc. P. N. Lebedev Inst.*, **196**, 62 (1989).
[2] D. L. Windt, *Computers in Physics*, **12**, 360 (1998).
[3] L. M. Brechovsky, *Waves in Stratified Media*, AN SSSR Publishers, Moscow 1957.
[4] A.G. Fedorov, *MRS 1999 Fall Meeting, Symposium B Abstract Book*, # B5.15, Boston 1999.
[5] B.L. Henke, E.M. Gullikson, J.C. Davis, *Atomic Data and Nuclear Data Tables*, **54**, 181 (1993).
[6] R.S. Rosen, D.G. Stearns, M.E. Kassner, J.-I. Koike, Y .Cheng, and S.P. Vernon, *Nanostruct. Mater.*, **3**, 195 (1993).